Progress in Oceanography 186 (2020) 102392

Contents lists available at ScienceDirect

Progress in Oceanography

journal homepage: www.elsevier.com/locate/pocean

Atmospheric dimethyl sulfide and its significant influence on the sea-to-air flux calculation over the Southern Ocean

Miming Zhang[a,*], Ki-Tae Park[b], Jinpei Yan[a], Keyhong Park[c], Yanfang Wu[d], Eunho Jang[b,e], Wei Gao[f], Guobin Tan[f,g], Jianjun Wang[a], Liqi Chen[a]

[a] Key Laboratory of Global Change and Marine-Atmospheric Chemistry, Third Institute of Oceanography, Ministry of Natural Resources, Siming District, Xiamen, Fujian 361005, PR China
[b] Division of Polar Climate Sciences, Korea Polar Research Institute, Incheon 21990, South Korea
[c] Division of Polar Ocean Science, Korea Polar Research Institute, Incheon 21990, South Korea
[d] School of Chemistry, Australian Centre for NanoMedicine and Australian Research Council (ARC) Centre of Excellence in Convergent Bio-Nano Science and Technology, The University of New South Wales, Sydney NSW 2052, Australia
[e] University of Science and Technology, 217 Gajeong-ro, Yuseong-gu, Daejeon 34113, South Korea
[f] Institute of Mass Spectrometry and Atmospheric Environment, Jinan University, Tianhe District, Guangzhou, Guangdong 510632, PR China
[g] Guangzhou Hexin Instrument Co., Ltd., Huangpu District, Guangzhou, Guangdong 510663, PR China

ARTICLE INFO

Keywords:
Dimethyl sulfide
Southern Ocean
Atmospheric DMS
Seawater DMS
DMS sea-to-air flux

ABSTRACT

Our understanding about the atmospheric dimethyl sulfide (DMS) and its influence to sea-to-air flux calculation in the Southern Ocean is still limited due to insufficient investigations. Herein, high-resolution shipboard underway simultaneous surface seawater and atmospheric DMS measurements were conducted in the Southern Ocean from February 23 to March 31, 2018. A larger variation of DMS levels was found in atmosphere compared with that in seawater. Remarkably, a large-scale area with high seawater and atmospheric DMS concentrations up to 27.9 nM and 3.92 ppbv, respectively, was investigated outside of Ross Sea sector. Atmospheric DMS levels were strongly impacted by wind speed and air mass convection. The relationship between atmospheric DMS and air mass exposure to oceanic chlorophyll varied greatly depending on the area of investigation. Some other regions with high DMS production capacity were examined as well beside those along the cruise tracks based on the results of positive correlations with high slopes and back trajectories. Moreover, significant uncertainty of sea-to-air DMS flux over the Southern Ocean could be caused by follows: (1) the selecting of different gas transfer coefficients; (2) the negative flux values calculated under high atmospheric DMS levels together with low seawater DMS concentrations; and (3) the greatly overestimated flux, approximately 47.1–76.9%, without considering the atmospheric DMS. This study highlights the urgent demand of high-resolution observations of atmospheric DMS over the Southern Ocean to estimate DMS emission with high accuracy.

1. Introduction

Dimethyl sulfide (DMS), which is mainly produced by marine phytoplankton, is the most abundant form of biogenic sulfur compounds released from the ocean (Stefels et al., 2007). Moreover, DMS is an important short-lived biogenic gas (Liss et al., 2014) and has been hypothesized that can affect cloud condensation nuclei (CCN) and cloud formation (Charlson et al., 1987). The Southern Ocean (south of 40°S) is a significant source for DMS (Kettle et al., 1999), the contribution of which was estimated to be approximately 5.8 Tg S a^{-1} (Global annual DMS emission was about 28.1 Tg S a^{-1}) (Lana et al., 2011). Seasonality of aerosol optical depth (AOD) (Gabric et al., 2005) and CCN (Vallina et al., 2006; Quinn et al., 2017) over the Southern Ocean are considered to be mainly related to DMS emissions. However, whether or not DMS can control the CCN number is still under debate (Quinn and Bates, 2011). Nonetheless, the Southern Ocean is a nice place to investigate how oceanic DMS impacts atmospheric sulfur compounds and, thereby, CCN, clouds and the climate.

Previously surface seawater DMS has been investigated in the Southern Ocean (see (Lana et al., 2011) and the National Oceanographic and Atmospheric Administration (NOAA) - Pacific Marine Environmental Laboratory (PMEL) database, http://saga.pmel.noaa.gov.dms). Significant change in surface water DMS concentration in the Southern Ocean over time scales of days to weeks at sub-km spatial

* Corresponding author.
E-mail address: zhangmiming@tio.org.cn (M. Zhang).

https://doi.org/10.1016/j.pocean.2020.102392
Received 20 July 2019; Received in revised form 26 March 2020; Accepted 7 June 2020
Available online 10 June 2020
0079-6611/

scales was first reported by Tortell and Long (2009). Similar phenomena were also found in the Ross Sea (Tortell et al., 2011), Amundsen Sea (Kim et al., 2017; Tortell et al., 2012) and marginal sea ice zone (Zhang et al., 2017). However, regarding atmospheric DMS measurements, only some discrete data points were obtained over the Southern Ocean (Inomata et al., 2006; Jones et al., 1998; Lee et al., 2010; Staubes and Georgii, 1993; Yokouchi et al., 1999) and Antarctic research stations (Berresheim et al., 1998; Preunkert et al., 2007; Read et al., 2008). Notably, by using a membrane equilibrator coupled with an atmospheric pressure chemical ionization mass spectrometer (APCI-MS) and a second APCI-MS (Saltzman et al., 2009), Bell et al. (2015) obtained a high-resolution seawater and atmospheric DMS dataset near east New Zealand (approximately 43°S–45°S). However, such observations in the Southern Ocean are still lacking.

As phytoplankton biomass, which is expressed here as chlorophyll, is considered to be related to seawater DMS production (Simo and Dachs, 2002; Yang et al.,2012), the relationship between phytoplankton biomass and atmospheric DMS has been analyzed in previous studies (Park et al., 2013; Preunkert et al., 2007). However, these studies generally used mean satellite-derived chlorophyll values in a selected region for discussion, which may introduce uncertainty if the air mass transported through an ocean presents a large phytoplankton biomass variability (e.g., the Southern Ocean (Arrigo et al., 1998)). Arnold et al. (2010) introduced a new method to calculate the air mass exposure to oceanic chlorophyll (E_{chl}), which provides a good index for the oceanic biogenic gas production capacity through which air mass has passed. Recently, by using this method to analyze atmospheric DMS collected over the Zeppelin Mountains in Svalbard (78.5°N, 11.8°E), Park et al. (2018) found that the DMS production capacity in the Greenland Sea was significantly higher than that in the Barents Sea, although phytoplankton biomass in the Barents Sea was more abundant.

The surface ocean DMS emissions (F, flux) are calculated by using $F = k\,\Delta C$, where k is the transfer velocity and ΔC is the difference of sea-air DMS concentration. Most of the Previous DMS flux calculation was performed without considering the influence of air DMS because of the measurement of DMS in atmosphere is far less than that in seawater (Lana et al, 2011). However, by using this calculation method, the DMS flux would possibly be overestimated when the atmospheric DMS levels are high enough. For instance, in the Southern Ocean high atmospheric DMS levels, e.g. above 1 ppbv in (Staubes and Georgii, 1993), could be received which were released from hundreds nM of seawater. Thus, it is highly demanded to evaluate the influence of atmospheric DMS over the sea-to-air flux calculation for a better understanding of DMS emission in the Southern Ocean.

In this study, high-resolution shipboard underway surface seawater and atmospheric DMS measurements were performed during the Chinese 34th Antarctic Research Expedition. Characteristics of atmospheric DMS distribution and its factors were investigated. The relationship between seawater and atmospheric DMS along the cruise track was analyzed. Moreover, the relationship between atmospheric DMS and E_{chl} was studied. The influence of atmospheric DMS levels upon the sea-to-air flux calculation was carefully studied as well.

2. Materials and methods

2.1. Cruise information

Our measurements were performed on board the *R/V Xue Long* from February 23 – March 31, 2018 during 34th Chinese Antarctic Research Expedition. The ship tracks only showed the region south of 40°S (Fig. 1): leg 1 extended from the sea near New Zealand to Amundsen Sea from February 23 to March 4; leg 2 extended from Amundsen Sea to the sea near New Zealand from March 5 to March 31.

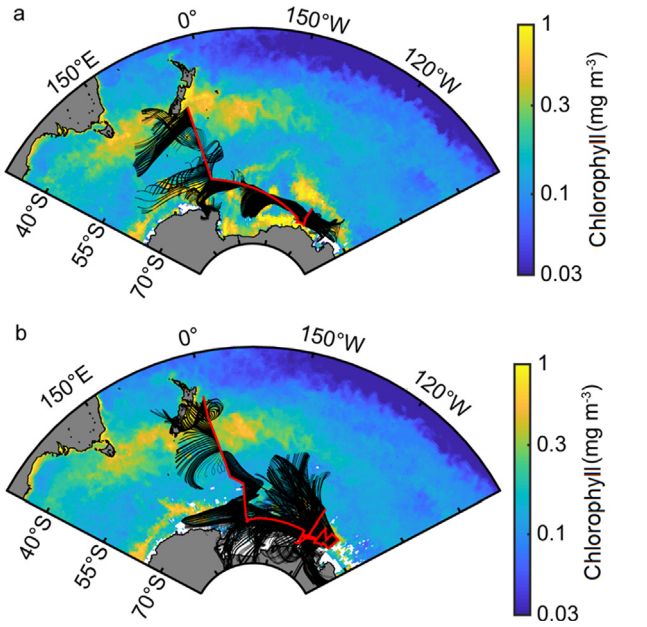

Fig. 1. Transects (red line) during the expedition. (a) leg 1, from February 23 to March 4, 2018; (b) leg 2, from March 5 to March 31. The background shows the eight day mean satellite-derived chlorophyll data in the period of February 18 - March 5, 2018 for leg 1 (a) and March 6 – April 6, 2018 for leg 2 (b). The black lines indicate the 2 day air mass back trajectories along the cruise tracks at an hourly interval. (For interpretation of the references to colour in this figure legend, the reader is referred to the web version of this article.)

2.2. Data sources (Seawater and atmospheric DMS, Chlorophyll, sea ice and meteorological Parameters)

A custom-made automatic purge and trap system coupled with a time-of-flight mass spectrometer (TOF-MS, SPI-MS 3000, Guangzhou Hexin Instrument Co., Ltd., China) was utilized for shipboard underway simultaneous measurements of atmospheric and seawater DMS (Zhang et al., 2019). Seawater and air samples could be continuously introduced into the system through the ship's seawater pump system at a depth of 4 m and air sampler inlet located at the front of ship at approximately 10 m above the sea surface, respectively. In every 10 min, a pair of one atmospheric and one seawater DMS data point can be obtained. Different volumes of DMS standard gas, such as 50, 100, 250, 500 and 1000 μL (5 ppmv, certified, Wuhanteqi Company, China) were used for calibration. Detection limits of atmospheric and seawater DMS were found to be 32 pptv and 0.07 nM (nmol L^{-1}).

E day chlorophyll data was achieved from the Level-3 product of Aqua Moderate Resolution Imaging Spectroradiometer at a 4 km resolution. Air mass back trajectories were calculated by the Hybrid Single-Particle Lagrangian Integrated Trajectories mode. Lifetime of atmospheric DMS is close to 2 days (Read et al., 2008); thus, the 2 day air mass back trajectories and hourly positions were adopted and combined with satellite-derived chlorophyll data to show the evolution of air mass exposure to phytoplankton biomass along the tracks. Other parameters, such as sea surface temperature (SST), salinity (SSS), phytoplankton biomass intensity (fluorescence), air temperature, air pressure and wind speed, were obtained from shipboard underway conductivity-temperature-depth (CTD) system (SBE21, USA) and meteorological observation system (Figure S1). The data of sea ice was obtained from the University of Bremen (https://seaice.uni-bremen.de/sea-ice-concentration), with a spatial resolution of 3.125 km × 3.125 km (Spreen et al., 2008).

2.3. Calculation of E_{chl}

The method to calculate E_{chl} was similar to that in the previous study of Park et al. (2018). Chlorophyll concentration in surface ocean area and the contact period of time when air mass travelled were the two main factors impacting the air mass DMS mixing ratio (Arnold et al., 2010; Park et al., 2018). The calculated E_{chl} here reflects the influences of phytoplankton biomass and atmospheric DMS oxidation on the DMS mixing ratio of air reaching the ship. The E_{chl} for each atmospheric DMS data point was calculated using the Eq. (1) as follows:

$$E_{Chl} = \frac{\sum_{t=1}^{48} Chl_t \bullet Chl_t \bullet e^{-\alpha\left(\frac{t}{24}\right)}}{n} \quad (1)$$

Here, Chl_t represents a 8 day mean chlorophyll concentration along the air mass back trajectory at a given time point (t = 1 to t = 48), and n represents the total number of time points that chlorophyll values are available. The term $e^{-\alpha(t/24)}$ is related to the normalization of photodecay, where α represents decay constant for DMS in the atmosphere due to photochemical oxidation process. The value of α was chose to be 0.43 which indicates a 35% DMS loss per day based on the report by Leck and Persson (1996) in Arctic atmosphere.

2.4. The calculation method of the sea-to-air DMS fluxes

As noted above, ocean-atmosphere DMS fluxes were computed by using the following gas exchange model:

$$F = k\Delta C = k(C_w - -C_g/H) \quad (2)$$

where C_w and C_g represent seawater and atmospheric DMS concentrations, respectively. H is the temperature-dependent DMS solubility in seawater by using the following equation (Dacey et al., 1984):

$$ln\, H(atm\, L\, mol^{-1}) = -3547/T(°K) + 12.64 \quad (3)$$

The k is parameterized by the wind speed and physicochemical properties of surface seawater. Similar with previous estimations by Kettle and Andreae (2000) and Lana et al. (2011), we employed the k parameters from Liss and Merlivat (1986) (hereafter LM86, linear equation) and Nightingale et al. (2000) (hereafter N00, quadiratic equation) for the DMS sea-to-air flux calculation. The fluxes were calculated under a Schmidt number (Sc_{DMS}) of 600, that of DMS in freshwater at 25 °C according to Saltzman et al. (1993). As the height (Z) of where the wind speed measurements performed on the ship was approximately 27 m, we calibrated the wind speed to that at 10 m following the method performed by Hsu et al. (1994):

$$U_x/U_{10} = (Z_x/Z_{10})^p \quad (4)$$

where U_{10} and Ux are the wind speed at a height of 10 m and 27 m, respectively, and the p value is 0.11, as referred to the study by Hsu et al. (1994).

3. Results and discussion subsubsection

3.1. Seawater and atmospheric DMS distributions

During the expedition, not only was large variability in seawater DMS investigated but also a much stronger variation in atmospheric DMS was observed, as there were more regions with high atmospheric DMS levels (marked with HA) than high seawater DMS levels (marked with HS) (Fig. 2). After excluding the high values region data points (including HA and HS regions), the remainder data was defined as "residual data points" cluster for further discussion. The mean values of seawater DMS were 2.5 ± 4.0 nM (undetected – 27.9 nM, n = 1340) and 1.3 ± 1.1 nM (undetected – 8.9 nM, n = 3257) in leg 1 and leg 2, respectively. The respective atmospheric DMS levels in leg 1 and leg 2 were ranged from undetected to 3.92 ppbv (0.56 ± 0.56 ppbv, n = 1374) and from undetected to 1.81 ppbv (0.27 ± 0.23 ppbv, n = 3353). In contrast to the existing surface seawater data in PMEL database (only some discrete measurements, Fig. 2c, d), we have obtained numerous data points for seawater and atmospheric DMS in areas that were previously un-investigated for DMS in the Southern Ocean. Note that almost no data about atmospheric DMS in these areas has been reported so far.

It is worth mentioning that a large-scale region with both high seawater and atmospheric DMS levels, HS01 and HA01, was found outside of the Ross Sea sector from February 27 to March 2 (Fig. 2a, c). The area of high atmospheric DMS was larger than the area of high seawater DMS along the track. The mean seawater and atmospheric DMS levels, 6.2 ± 6.4 nM (n = 357) and 1.37 ± 0.56 ppbv (n = 367), respectively, were comparable with the high-resolution measurements over Atlantic Arctic Ocean where the observed mean value was 1459 ± 866 pptv under a relatively high seawater DMS condition (mean value was 8.63 ± 2.77 nM) (Marandino et al., 2008). The observed seawater DMS was lower than those of previous studies in spring and summer Southern Ocean (up to hundreds of nM) (Kim et al., 2017; Tortell et al., 2011), while the atmospheric DMS were much higher than those, general below 1 ppbv, in Curran et al. (1998), Inomata et al. (2006) and Staubes and Georgii (1993). The atmospheric DMS values decreased from HA01 to HA05, and the distributions of atmospheric DMS indicated a strong decreasing tendency from HA01 to the east and from low latitudes (HA03) to high latitudes (HA05) (Fig. 2 a, b; Fig. 3 a). DMS release from HS01 probably impacted those high atmospheric DMS concentrations based on the back trajectory results (Fig. 1).

3.2. Relationship between seawater and atmospheric DMS

Obviously, atmospheric DMS variability was not always coincide with seawater DMS variability (Fig. 3a). Most of the high atmospheric DMS data points were consistent with low seawater DMS levels, except HA07, HA08 and some parts of HA01. And this inconsistency was also found in other studies including the western Pacific Ocean (Marandino et al., 2013) and the Southern Ocean (Bell et al., 2015). Although several studies reported the variation tendency of atmospheric DMS followed by that of surface seawater DMS (Marandino et al., 2007; 2008; 2009), atmospheric DMS is also influenced by a number of other parameters, such as wind speed variability, air mass trajectories, atmospheric oxidation rates and boundary layer heights (Bell et al., 2013).

Wind speed is a critical factor that affects atmospheric DMS level by impacting the sea-to-air transfer velocity of surface seawater DMS (Liss and Merlivat, 1986). Taking the data in HA01 and HS01 as an example, under a relatively low wind speed (generally below ~9 m s^{-1}), an extremely strong relationship between seawater and atmospheric DMS (slope = 0.049, R^2 = 0.80, n = 140, Fig. 3b) was found, indicating that atmospheric DMS in this area was strongly related to its local seawater DMS releasing. As the wind speed increased from ~9 m s^{-1} to ~15 m s^{-1}, another relatively strong relationship between seawater and atmospheric DMS was found (slope = 0.091, R^2 = 0.37, n = 58); however, under extremely high wind speed conditions (above 15 m s^{-1}), the atmospheric DMS presented significant fluctuations with a small change in seawater DMS (below 3 nM). It is noticed that high seawater DMS levels (above 10 nM) were only found under low wind speeds (below ~ 9 m s^{-1}) (Fig. 3b). The high DMS levels were possibly caused by the following factors: (1) the high DMS production after the phytoplankton bloom in summer (high biomass intensity in Fig. 4a) (Stefels et al., 2007; Zhang et al., 2017), (2) low DMS bacterial consumption rate under low seawater temperature (mean value of 1.1 ± 0.9 °C (0–3.6 °C); from February 27 to March 2, 2018, n = 561, Figure S1) (Del Valle et al., 2009), (3) low seawater and atmospheric DMS photochemical oxidation rate in early fall caused by a low solar radiation dose (Vogt and Liss, 2009), and (4) relatively low sea-to-air

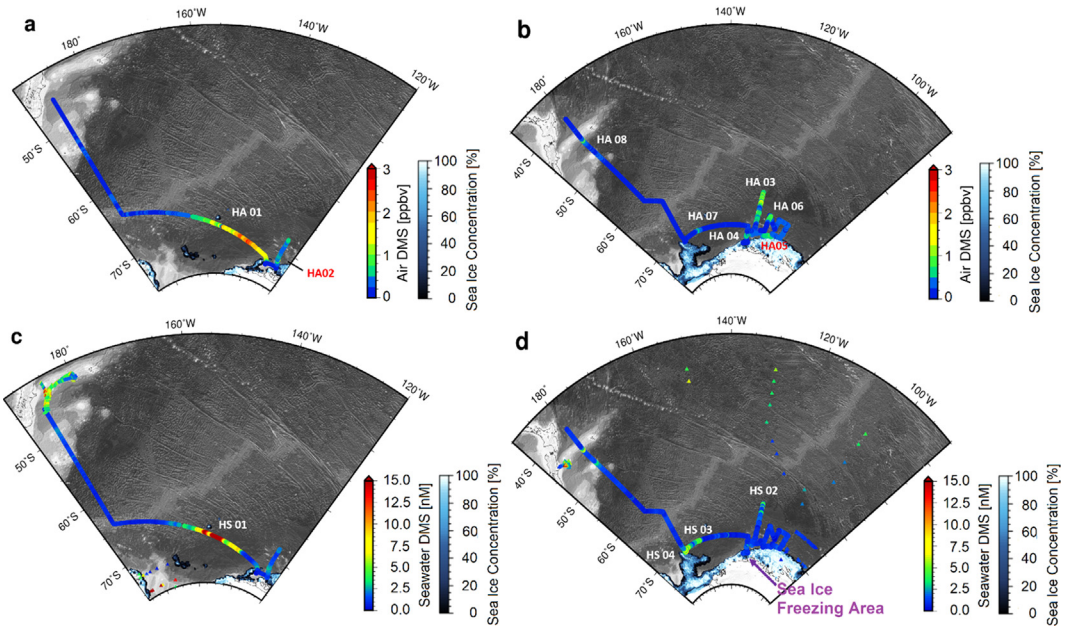

Fig. 2. Atmospheric and surface seawater DMS distributions along the leg 1 (a, c) and leg 2 (b, d). Note that regions with high atmospheric DMS concentrations (HA, generally above 0.5 ppbv) and high seawater DMS concentrations (HS, generally above 3 nM) were marked along the cruise track. The scales of air and seawater DMS were capped to 3 ppbv and 15 nM, respectively, to ensure readability. Historical seawater DMS data points are resented with triangles (c, d). Sea ice distributions on March 1, 2018, and March 16, 2018, were matched with the backgrounds of leg 1 (a, c) and leg 2 (b, d), respectively, because the ship was passing the sea ice cover region during those periods. The sea ice freezing area is marked with a purple arrow. (For interpretation of the references to colour in this figure legend, the reader is referred to the web version of this article.)

DMS exchange (Fig. 5 b, mean wind speed was 5.0 ± 1.0 m s^{-1}, mean DMS fluxes was 6.3 ± 4.7 μmol m^{-2} d^{-1}, n = 140; calculated by N2000). As the wind speed increased, the linear slope between air and seawater DMS increased, from 0.049 to 0.091, and seawater DMS concentrations also decreased in the region of HA01 and HS01, indicating that the sea-to-air exchange was possibly the main factor responsible for the reduction of seawater DMS during the observation period. Additionally, the R^2 value between atmospheric and seawater DMS decreased from 0.80 to 0.37, suggesting that local DMS emissions might not be the only main factor affecting atmospheric DMS. Another factor, i.e., air mass transportation, should be considered as well.

Cold (air temperature generally below 3 °C; Figure S1) and dark season at this high latitude (south of 60°S) could extend the lifetime of DMS (normally about 1 day (Kloster et al., 2006)) to approximately 2 days (Read et al., 2008), indicating that atmospheric DMS could be transported over a much longer distance than in spring and summer (when there is a higher solar radiation dose and longer daytime). The results of back trajectories suggested that air mass mixing process over the Southern Ocean might have a significant impact on atmospheric DMS concentration (Fig. 1). The air mass containing high DMS levels from HS01 and HA01 could be transported to the eastern side and affect atmospheric DMS distributions there. Moreover, air mass originated from the inland area and contained with very low atmospheric DMS concentrations (Preunkert et al., 2008) may decrease atmospheric DMS levels over the ocean.

Sea ice cover can strongly influence the relationship between seawater and atmospheric DMS (Fig. 3a). The sea-to-air DMS exchange was constrained by the sea ice cover under high wind speeds (general above ~ 15 m s^{-1}) and DMS levels (general above 5 nM) in HS04 (Figure S2). By contrast, in another region where sea ice was forming (Figure S3), low levels of both seawater and atmospheric DMS were observed (Fig. 2d). This large difference in seawater DMS level between these two areas might be explained by the change in maximum phytoplankton activity depth caused by the thickness growth of sea ice. The

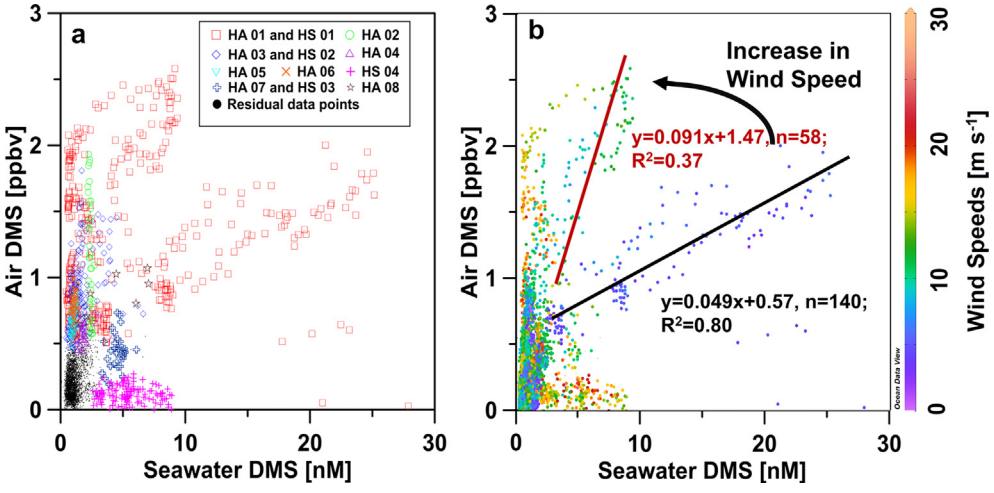

Fig. 3. (a) Patterns between seawater and atmospheric DMS in distinct regions. (b) The influence of wind speed on the relationship between seawater and atmospheric DMS. The black and brown line show linear relationship between seawater and atmospheric DMS at wind speeds below ~9 m s^{-1} and between ~9 m s^{-1} and ~ 15 m s^{-1}, respectively, in HA01 and HS01.

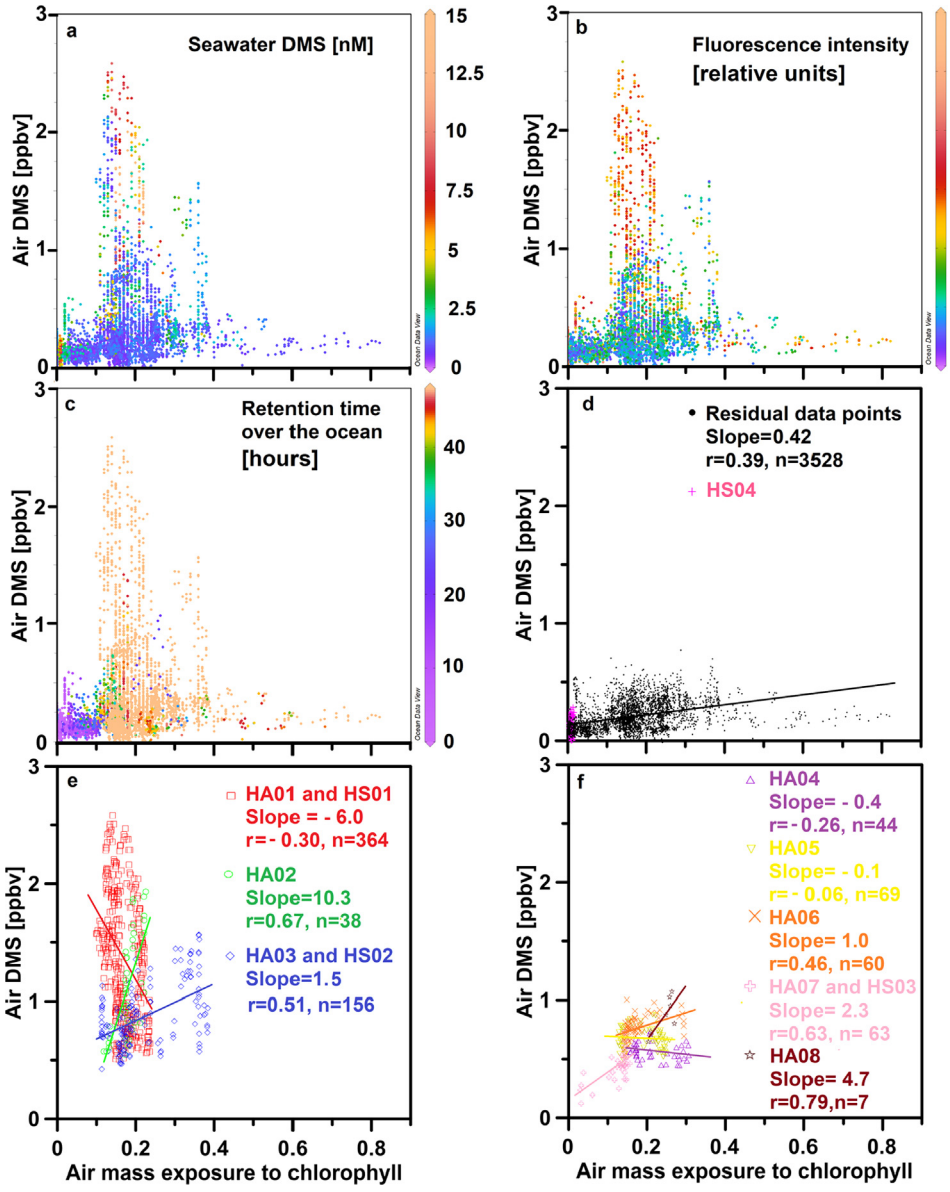

Fig. 4. Relationship between the atmospheric DMS and calculated air mass exposure to chlorophyll. All datasets were compared with (a) seawater DMS (the scale was the same as in Fig. 2), (b) underway surface water fluorescence intensity and (c) back trajectory retention time over the ocean. These correlations result in (d) HS04 (purple crosses) and the residual data points (black dots); in (e) HA01 and HS01 (red squares), HA02 (green circles), HA03 and HS02 (blue rhombuses), (f) HA04 (purple triangles,), HA05 (yellow inverted triangles), HA06 (orange X), HA07 and HS03 (pink crosses) and HA08 (brown stars). (For interpretation of the references to colour in this figure legend, the reader is referred to the web version of this article.)

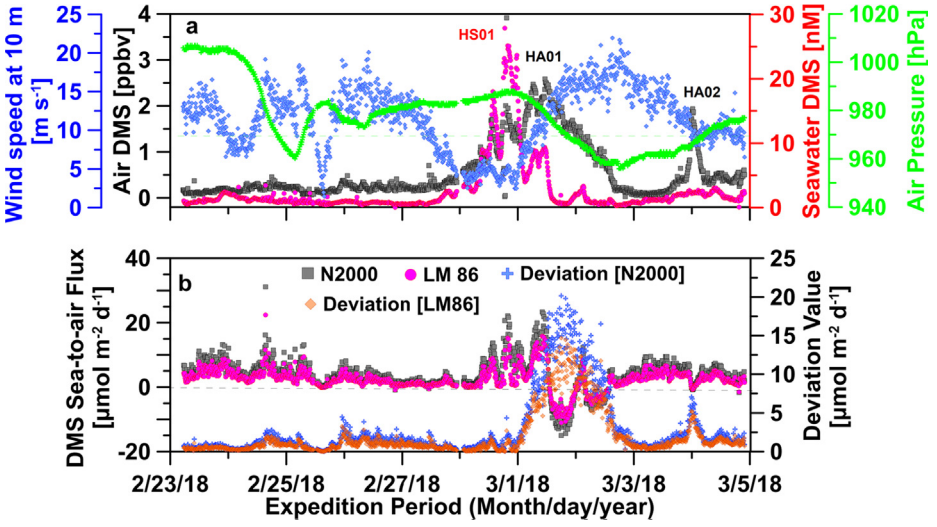

Fig. 5. (a) The variations of seawater (red) and atmospheric (black) DMS, wind speeds (blue) and air pressure (green) along the leg 1. Green dash line indicates the air pressure value of 970 hPa. (b) The DMS sea-to-air fluxes variations along the leg 1 by N2000 (grey square) and LM86 (red dots). The deviation value between without and with considering the atmospheric DMS were presented by blue cross (N2000) and orange diamond (LM86). Black dash line indicates the DMS flux value of 0 μmol m^{-2} d^{-1}. Note that the HA and HS regions were also marked in Fig. 2. (For interpretation of the references to colour in this figure legend, the reader is referred to the web version of this article.)

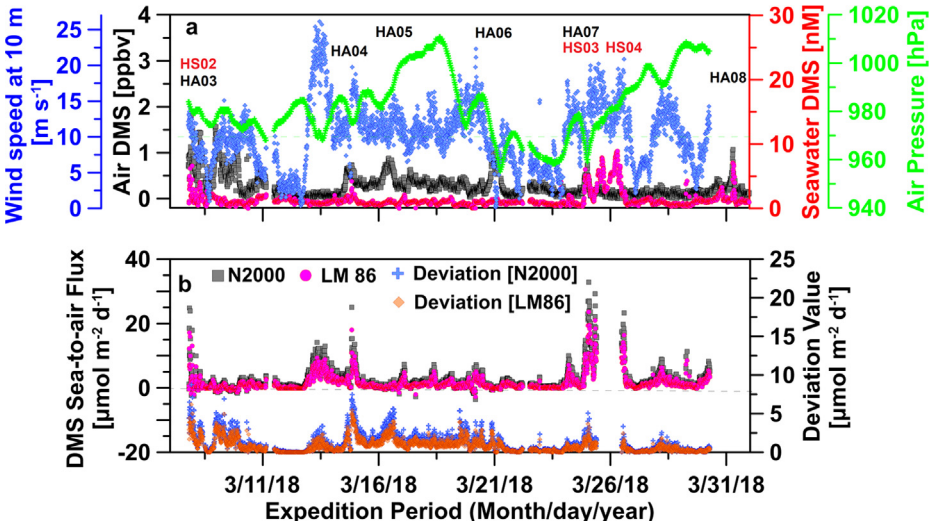

Fig. 6. (a) The variations of seawater (red) and atmospheric (black) DMS, wind speeds (blue) and air pressure (green) along the leg 2. Green dash line indicates the air pressure value of 970 hPa. (b) The DMS sea-to-air fluxes variations along the leg 2 by N2000 (grey square) and LM86 (red dots). The deviation value between without and with considering the atmospheric DMS were presented by blue cross (N2000) and orange diamond (LM86). Black dash line indicated the DMS flux value of 0 μmol m^{-2} d^{-1}. Noted that the DMS data in HS04 was removed due to the sea-to-air exchange of DMS was limited by heavy sea ice condition. Note that the HA and HS regions were also marked in Fig. 2. (For interpretation of the references to colour in this figure legend, the reader is referred to the web version of this article.)

suitable depth for phytoplankton growth changed from deeper water to a depth beneath the sea ice because the sea ice with increased thickness decreased the solar radiation intensity in the upper layer water. Therefore, phytoplankton organisms were likely to accumulate under the bottom of the sea ice and so high DMS levels could be observed there (Trevena and Jones, 2012).

3.3. Linking atmospheric DMS with E_{chl}

Because both the air mass transportation history and biological activities of the ocean region significantly impact the atmospheric DMS levels, we calculated the E_{chl} to indicate the DMS source intensity along the trajectories for the following discussion. More explicitly, the slope between atmospheric DMS and E_{chl} was approximately corresponded to the DMS production capacity of the ocean region (Park et al., 2018). Generally, it was very difficult to find a linear relationship between atmospheric DMS and E_{chl} under a full dataset (Fig. 4a). However, when data were analysed separately in distinct regions, as investigated in section 3.2, then these correlations generated interesting results that are worth careful interpretation.

Weak negative correlations, r = − 0.30 (n = 364, slope = − 6.0) and r = − 0.26 (n = 44, slope = − 0.4), and no correlations (r = -0.06, slope = − 0.1, n = 69) between atmospheric DMS and E_{chl} were found in regions of HA01 and HS01, HA04 and HA05 respectively (Fig. 4e, f). These results were different from the positive results from the continental research station in the Arctic (Park et al., 2018) and from other datasets along the legs. The insignificant correlations may be attributed to a stronger influence of localized DMS emission on atmospheric DMS than that of a 2 day biological exposure under high wind speed condition (average wind speed in HA01, HA04 and HA05 were 11.2 ± 6.0 m s^{-1} (n = 367), 13.5 ± 4.8 m s^{-1} (n = 50) and 12.8 ± 2.1 m s^{-1} (n = 69)).

The DMS production capacity of ocean area varied greatly depending on the area of investigation. Weak positive correlations were found in HA03 and HS02 (r = 0.52, p < 0.05, n = 140) and HA06 (r = 0.42, p < 0.05, n = 60), and significant positive correlations between atmospheric DMS and E_{chl} were found in HA02 (r = 0.67, p < 0.05, n = 38), HA07 and HS04 (r = 0.63, p < 0.05, n = 63) and HA08 (r = 0.79, p < 0.05, n = 7). The slope values ranged from 10.3 to 1.9 indicated a large variation of oceanic DMS production capacity in the Southern Ocean during the fall. The extremely high slope value in HA02 can be easily explained by the influence of a significant DMS emission from HS01 according to the back trajectories. However, the results in HA03 and HA06 suggested high DMS production capacity regions possibly existed in the northern part of HS01 as some back trajectories crossed there with high chlorophyll levels (Fig. 1). For the results of HA07 and HA08, in the meantime, it was observed for small scales high seawater DMS levels of approximately 5 nM in the marginal sea ice zone and along the subtropical front. The observed high DMS levels in these two regions were consistent with our previous findings in Prydz Bay during the sea ice freezing period and along the subtropical front in March in western Austria (Zhang et al., 2017). Additionally, the slope in HA08 (r = 4.7) was larger than that in HA07 and HS04 (r = 2.3), indicating that the DMS production capacity along subtropical front might be greater. Although the DMS levels in these two regions were similar, the area of high DMS production along subtropical front, as identified with high chlorophyll levels, was much larger than that in HS03 (Fig. 1b).

Finally, a weak positive correlation, r = 0.39 (p < 0.05, n = 3528, Fig. 4d), was found between atmospheric DMS and E_{chl} in the residual data points groups. Although some data points were calculated from the air mass back trajectories passing over sea ice cover and Antarctic inland area (Fig. 4c) which could not be used to reflect oceanic DMS production capacity, the obtained value of a low linear slope of 0.42 indicated that seawater DMS production capacity in most regions of the Southern Ocean during the fall was lower than those of high HA regions. Even under high biomass and E_{chl} conditions (> 0.6, Fig. 4b), both air and seawater DMS exhibited low levels (Fig. 4a). This result might be explained by two major factors: (1) low dimethylsulfoniopropionate (DMSP) contained phytoplankton species, like the *Diatom* (Boyd, 2002; Kim et al., 2017); and (2) the DMS production rate not being very high over there.

3.4. The results of DMS sea-to-air flux calculation

The results for the DMS sea-to-air flux calculation were presented in Fig. 5(b) and Fig. 6(b). Significant variations in the flux were found in both legs. However, the DMS flux variations were not always consistent with those of seawater DMS and wind speeds. The mean fluxes calculated by seawater and atmospheric DMS were 3.8 ± 4.9 μmol m^{-2} d^{-1} (−15.0 to 31.1 μmol m^{-2} d^{-1}, n = 1340, N2000) and 2.6 ± 3.5 μmol m^{-2} d^{-1} (−10.9 to 22.6 μmol m^{-2} d^{-1}, n = 1340, LM86) in leg 1; and were 2.4 ± 3.5 μmol m^{-2} d^{-1} (−3.6 to 32.8 μmol m^{-2} d^{-1}, n = 2881, N2000) and 1.7 ± 2.5 μmol m^{-2} d^{-1} (−2.6 to 23.8 μmol m^{-2} d^{-1}, n = 2881, LM86) in leg 2. These mean values were comparable with the findings by Curran and Jones (2000) where the DMS fluxes in spring were 3.8 μmol m^{-2} d^{-1} and 1.7 μmol m^{-2} d^{-1} in the Subantarctic Zone and Antarctic Zone respectively, but much lower with those results in spring and summer of polynyas (e.g. above 20 μmol m^{-2} d^{-1} in (Tortell et al., 2011, 2012;

Kim et al., 2017)). In addition to this, the DMS fluxes were also calculated by neglecting the atmospheric DMS, and the mean fluxes were 6.7 ± 4.9 μmol m^{-2} d^{-1} (0.1 to 35.5 μmol m^{-2} d^{-1}, n = 1340, N2000) and 4.6 ± 3.6 μmol m^{-2} d^{-1} (under detected – 24.3 μmol m^{-2} d^{-1}, n = 1340, LM86) in leg 1; and were 3.5 ± 3.9 μmol m^{-2} d^{-1} (under detected – 35.3 μmol m^{-2} d^{-1}, n = 2881, N2000) and 2.5 ± 2.8 μmol m^{-2} d^{-1} (under detected – 25.6 μmol m^{-2} d^{-1}, n = 2881, LM86) in leg 2. Generally, the calculation results by N2000 were higher (approximately 40.0–46.2% calculated by the difference of mean values) than those by LM86 due to that the *k* value of N2000 is higher than that of LM86 under the high wind speed (> 10 m s^{-1}) over the Southern Ocean. As reported in Elliott (2009), large differences in estimating DMS fluxes by employing various gas exchange models were investigated, it is possibly that estimations of DMS emission over the Southern Ocean vary greatly by using different *k* parameterizations.

It is worth to point out that a dataset of negative DMS flux values, low to −15.0 μmol m^{-2} d^{-1} (N2000) and −10.9 μmol m^{-2} d^{-1} (LM86), was obtained in leg 1 (Fig. 5b). As discussed above, a high air DMS concentration could be transported to an area of a very low seawater DMS level because the lifetime of DMS in the remote marine atmosphere has been estimated to be ~2 days (Read et al., 2008). In this case, the calculated C_g/H were larger than the seawater DMS concentrations, and thus, negative ΔC were obtained. In contrast, these negative results were unexpected compared with the common sense that DMS sea-to-air flux calculation result is always positive as the C_g/H is neglected in the calculation. The negative values indicated that the relative high air DMS levels could possibly re-dissolve into the seawater with low DMS concentrations. However, this kind of phenomena might be rare to occur as the DMS in natural seawater is generally saturated.

The great difference of DMS flux calculation between with and without considering the atmospheric DMS was investigated (deviation values in Fig. 5b and b). The mean deviation values were 2.9 ± 4.0 μmol m^{-2} d^{-1} (0 – 20.2 μmol m^{-2} d^{-1}, n = 1340, N2000) and 2.0 ± 2.9 μmol m^{-2} d^{-1} (0–14.7 μmol m^{-2} d^{-1}, n = 1340, LM86) in leg 1; and were 1.2 ± 1.2 μmol m^{-2} d^{-1} (0–8.7 μmol m^{-2} d^{-1}, n = 2881, N2000) and 0.8 ± 0.8 μmol m^{-2} d^{-1} (0–6.2 μmol m^{-2} d^{-1}, n = 2881, LM86) in leg 2. The largest deviation values occurred in the relatively high atmospheric DMS levels together with low seawater DMS concentrations and relatively high wind speeds (> 10 m s^{-1}) in leg 1 (Fig. 5b). The difference between these mean deviation values and DMS flux (calculated by seawater and atmospheric DMS) suggested that the DMS flux values calculated without the atmospheric DMS were approximately 47.1% − 76.9% overestimated over the fall of Southern Ocean. In this case, significant influence of atmospheric DMS to the sea-to-air flux calculation by using the two-layer model (Liss and Slater, 1974) over the Southern Ocean was investigated.

Generally, the factors that might cause the uncertainty for flux estimation were discussed here as follows. Firstly, in terms of selecting *k* parameterization, especially for those in high wind speed (> 10 m s^{-1}), *k* value varies significant (Ho et al., 2006). Additionally, gas transfer coefficients calculated by the eddy covariance in the high wind speed of Southern Ocean were also limited and uncertain (Bell et al., 2015). A suitable *k* parameterization for the DMS sea-to-air calculation over the Southern Ocean should be further investigated. Secondly, the calculated negative flux values should trigger more attentions as the phenomena of high atmospheric DMS levels transported to low seawater DMS regions is supposed to be quite common in the Southern Ocean. However, to the best of our knowledge, almost all previous estimations, e.g. in Kettle and Andreae (2000) and Lana et al. (2011), did not notice this issue. Thirdly, because the observed atmospheric DMS data over the Southern Ocean is extremely insufficient, the results of DMS flux estimated without considering atmospheric DMS would greatly overestimate the DMS emission over there, particularly in the region of polynyas and marginal sea ice zone, where extremely high seawater DMS levels were observed. Therefore, high-resolution observations of atmospheric DMS are urgently required to obtain a better understanding of DMS emissions in these areas.

4. Conclusions and implication

High-resolution measurements of surface seawater and atmospheric DMS during the 34th Chinese Antarctic Research Expedition from February 23 to March 31, 2018, were performed in the Southern Ocean. We found much stronger variability in atmospheric DMS level than that in surface seawater level. A large-scale region with high levels of seawater and atmospheric DMS (up to 27.9 nM and 3.92 ppbv, respectively) was investigated outside of the Ross Sea sector. The influences of seawater DMS, wind speed, air mass transportation and sea ice cover on the atmospheric DMS were examined. DMS production capacity of the Southern Ocean was lower during expedition time than productive spring-summer time (i.e., lower sea surface DMS concentrations, lower slopes between atmospheric DMS and biological exposure), and varied greatly from region to region. High atmospheric DMS concentrations were possibly related to several hotspots of oceanic DMS under high wind speed events. Additionally, significant influence for atmospheric DMS on the calculation of sea-to-air flux was investigated. It is likely that DMS emissions over the Southern Ocean estimated by nearly all previous studies were overestimated. Also further attentions should be drawn on the improvement about the investigations of gas transfer coefficient and the sea-to-air calculation model. This study provides the insight about how oceanic DMS impacts atmospheric DMS in the Southern Ocean and the findings from this study could be further utilized to analyze how oceanic DMS impacts sulfur aerosols and subsequently, particle formation and CCN.

Data availability

All data needed to draw the conclusions in the present study are shown in this paper and/or the Supplementary Materials. For additional data related to this study, please contact the corresponding author (zhangmiming@tio.org.cn).

Author contributions

M.M.Z. and J.P.Y. initiated and led the study. K.T.P and E.J. conducted the calculation of Echl. L.Q.C., L.Q., K.P., Y.F.W., J.J.W. W.G. involved the discussion and revision.

Acknowledgments

We thank the Chinese Arctic and Antarctic Administration (CAA) of Ministry of Natural Resources and the crew of R/V Xue Long for their support with field operations. This work was supported by the National Natural Science Foundation of China (NSFC) (41706104, 41941014), the international cooperation program managed by the National Research Foundation of South Korea (NRF-2019K2A9A2A06025329) and NSFC (41911540471), the Qingdao National Laboratory for Marine Science and Technology Foundation (No. QNLM2016ORP0109), the Ministry of Science and Technology and Key Research & Development Programs (No. 2018YFC1406703), the Chinese Projects for Investigations and Assessments of the Arctic and Antarctic (CHINARE2017-2020), the response and feedback of the Southern Ocean to climate change (RFSOCC2020-2025), the International Organizations and Conference and Bilateral Cooperation of Maritime Affairs, the Scientific Research Foundation of Third Institute of Oceanography, at the Ministry of Natural Resources (under contract No. 2019009, No. 2018014), and the Korean Polar Research Institute (Grant PE20140, PE 20060).

Appendix A. Supplementary material

Supplementary data to this article can be found online at https://

doi.org/10.1016/j.pocean.2020.102392.

References

Arnold, S.R., Spracklen, D.V., Gebhardt, S., Custer, T., Williams, J., Peeken, I., Alvain, S., 2010. Relationships between atmospheric organic compounds and air-mass exposure to marine biology. Environ. Chem. 7 (3), 232–241. https://doi.org/10.1071/EN09144.

Arrigo, K.R., Worthen, D., Schnell, A., Lizotte, M.P., 1998. Primary production in Southern Ocean waters. J Geophys Res-Oceans 103 (C8), 15587–15600. https://doi.org/10.1029/98JC00930.

Bell, T., De Bruyn, W., Miller, S., Ward, B., Christensen, K., Saltzman, E.S., 2013. Air–sea dimethylsulfide (DMS) gas transfer in the North Atlantic: evidence for limited interfacial gas exchange at high wind speed. Atmos. Chem. Phys. 13 (21), 11073–11087. https://doi.org/10.5194/acp-13-11073-2013.

Bell, T.G., De Bruyn, W., Marandino, C.A., Miller, S.D., Law, C.S., Smith, M.J., Saltzman, E.S., 2015. Dimethylsulfide gas transfer coefficients from algal blooms in the Southern Ocean. Atmos. Chem. Phys. 15 (4), 1783–1794. https://doi.org/10.5194/acp-15-1783-2015.

Berresheim, H., Huey, J.W., Thorn, R.P., Eisele, F.L., Tanner, D.J., Jefferson, A., 1998. Measurements of dimethyl sulfide, dimethyl sulfoxide, dimethyl sulfone, and aerosol ions at Palmer Station, Antarctica. J. Geophys. Res. 103 (D1), 1629–1637. https://doi.org/10.1029/97JD00695.

Boyd, P.W., 2002. Environmental factors controlling phytoplankton processes in the Southern Ocean. J. Phycol. 38 (5), 844–861. https://doi.org/10.1046/j.1529-8817.2002. t01-1-01203.x.

Charlson, R.J., Lovelock, J.E., Andreaei, M.O., Warren, S.G., 1987. Oceanic phytoplankton atmospheric sulphur, cloud albedo and climate. Nature 326 (6114), 655–661. https://doi.org/10.1038/326655a0.

Curran, M.A.J., Jones, G.B., Burton, H., 1998. Spatial distribution of dimethylsulfide and dimethylsulfoniopropionate in the Australasian sector of the Southern Ocean. J. Geophys. Res. 103 (D13), 16677–16689. https://doi.org/10.1029/97JD03453.

Curran, M.A.J., Jones, G.B., 2000. Dimethyl sulfide in the Southern Ocean: Seasonality and flux. J. Geophys. Res. 10520 (D16451–420), 459. https://doi.org/10.1029/2000JD900176.

Dacey, J.W.H., Wakeham, S.G., Howes, B.L., 1984. Henry's law constants for dimethylsulfide in freshwater and seawater. Geophys. Res. Lett. 11 (10), 991–994. https://doi.org/10.1029/GL011i010p00991.

Del Valle, D.A., Kieber, D.J., Toole, D.A., Brinkley, J., Kiene, R.P., 2009. Biological consumption of dimethylsulfide (DMS) and its importance in DMS dynamics in the Ross Sea Antarctica. Limnol Oceanogr. 54 (3), 785–798. https://doi.org/10.4319/lo.2009.54. 3.0785.

Gabric, A.J., Shephard, J.M., Knight, J.M., Jones, G., Trevena, A.J., 2005. Correlations between the satellite-derived seasonal cycles of phytoplankton biomass and aerosol optical depth in the Southern Ocean: Evidence for the influence of sea ice. Global Biogeochem. Cy. 19 (4), GB4018. https://doi.org/10.1029/2005gb002546.

Elliott, S., 2009. Dependence of DMS global sea-air flux distribution on transfer velocity and concentration field type. J. Geophys. Res.Biogeosci. 114 (G2). https://doi.org/10.1029/2008JG000710.

Ho, D.T., Law, C.S., Smith, M.J., Schlosse, P.R., Harvey, M., Hill, P., 2006. Measurements of air-sea gas exchange at high wind speeds in the Southern Ocean: Implications for global parameterizations. Geophys. Res. Lett. 33 (16), L16611. https://doi.org/10.1029/2006 gl026817.

Hsu, S.A., Meindl, E.A., Gilhousen, D.B., 1994. Determining the power-law wind-profile exponent under near-neutral stability conditions at sea. J. Appl. Meteorol. 33 (6), 757–765. https://doi.org/10.1175/1520-0450(1994)033<0757:DTPLWP>2.0.CO;2.

Inomata, Y., Hayashi, M., Osada, K., Iwasaka, Y., 2006. Spatial distributions of volatile sulfur compounds in surface seawater and overlying atmosphere in the northwestern Pacific Ocean, eastern Indian Ocean, and Southern Ocean. Global Biogeochem. Cycles 20 (2), GB2022. https://doi.org/10.1029/2005GB002518.

Jones, G.B., Curran, M.A.J., Swan, H.B., Greene, R.M., Griffiths, F.B., Clementson, L.A., 1998. Influence of different water masses and biological activity on dimethylsulphide and dimethylsulphoniopropionate in the subantarctic zone of the Southern Ocean during ACE 1. J. Geophys. Res.-Atmospheres 103 (D13), 16691–16701. https://doi.org/10.1029/98JD01200.

Kettle, A., Andreae, M., Amouroux, D., Andreae, T., Bates, T., Berresheim, H., Bingemer, H., Boniforti, R., Curran, M., DiTullio, G., 1999. A global database of sea surface dimethylsulfide (DMS) measurements and a procedure to predict sea surface DMS as a function of latitude, longitude, and month. Global Biogeochem. Cy. 13 (2), 399–444. https://doi.org/10.1029/1999gb900004.

Kettle, A., Andreae, M., 2000. Flux of dimethylsulfide from the oceans: A comparison of updated data sets and flux models. J. Geophys. Res. 10526 (D22793–726), 808. https://doi.org/10.1029/2000JD900252.

Kim, I., Hahm, D., Park, K., Lee, Y., Choi, J.O., Zhang, M., Chen, L., Kim, H.C., Lee, S., 2017. Characteristics of the horizontal and vertical distributions of dimethyl sulfide throughout the Amundsen Sea Polynya. Sci. Total Environ. 584, 154–163. https://doi.org/10.1016/j.scitotenv.2017.01.165.

Kloster, S., Feichter, J., Maier-Reimer, E., Six, K.D., Stier, P., Wetzel, P., 2006. DMS cycle in the marine ocean-atmosphere system? a global model study. Biogeosciences 3 (1), 29–51. https://doi.org/10.5194/bgd-2-1067-2005.

Lana, A., Bell, T., Simó, R., Vallina, S.M., Ballabrera-Poy, J., Kettle, A., Dachs, J., Bopp, L., Saltzman, E., Stefels, J., 2011. An updated climatology of surface dimethlysulfide concentrations and emission fluxes in the global ocean. Global Biogeochem. Cy. 25 (1), GB1004. https://doi.org/10.1029/2010GB003850.

Leck, C., Persson, C., 1996. Seasonal and short-term variability in dimethyl sulfide, sulfur dioxide and biogenic sulfur and sea salt aerosol particles in the arctic marine boundary layer during summer and autumn. Tellus B 48 (2), 272–299. https://doi.org/10.1034/j.1600-0889.48.issue2.1.x.

Lee, G., Park, J., Jang, Y., Lee, M., Kim, K.R., Oh, J.R., Kim, D., Yi, H.I., Kim, T.Y., 2010. Vertical variability of seawater DMS in the South Pacific Ocean and its implication for atmospheric and surface seawater DMS. Chemosphere 78 (8), 1063–1070. https://doi.org/10.1016/j.chemosphere.2009.10.054.

Liss, P.S., Slater, P.G., 1974. Flux of Gases across the Air-Sea Interface. Nature 247 (5438), 181–184. https://doi.org/10.1038/247181a0.

Liss, P. S., and Merlivat, L., 1986, Air-sea gas exchange rates: Introduction and synthesis, in: The role of air-sea exchange in geochemical cycling, edited by: Buatmenard, P., Reidel, 185, 113-127. doi: 10.1007/978-94-009-4738-2_5.

Liss, P.S., Marandino, C.A., Dahl, E.E., Helmig, D., Hintsa, E.J., Hughes, C., Johnson, M.T., Moore, R.M., Plane, J.M., Quack, B., 2014. Short-lived trace gases in the surface ocean and the atmosphere, in Ocean-Atmosphere Interactions of Gases and Particles, 1–54. Springer. https://doi.org/10.1007/978-3-642-25643-1_1.

Marandino, C., De Bruyn, W., Miller, S., Saltzman, E., 2007. Eddy correlation measurements of the air/sea flux of dimethylsulfide over the North Pacific Ocean. J. Geophys. Res. 112, D03301. https://doi.org/10.1029/2006JD007293.

Marandino, C., De Bruyn, W., Miller, S., Saltzman, E., 2008. DMS air/sea flux and gas transfer coefficients from the North Atlantic summertime coccolithophore bloom. Geophys. Res. Lett. 35 (23), L23812. https://doi.org/10.1029/2008GL036370.

Marandino, C., De Bruyn, W., Miller, S., Saltzman, E., 2009. Open ocean DMS air/sea fluxes over the eastern South Pacific Ocean. Atmos. Chem. Phys. 9 (2), 345–356. https://doi.org/10.5194/acp-9-345-2009.

Marandino, C., Tegtmeier, S., Krüger, K., Zindler, C., Atlas, E., Moore, F., Bange, H.W., 2013. Dimethylsulphide (DMS) emissions from the western Pacific Ocean: a potential marine source for stratospheric sulphur? Atmos. Chem. Phys. 13 (16), 8427–8437. https://doi.org/10.5194/acp-13-8813-2013.

Nightingale, P.D., Malin, G., Law, C.S., Watson, A.J., Liss, P.S., Liddicoat, M.I., Boutin, J., Upstill-Goddard, R.C., 2000. In situ evaluation of air-sea gas exchange parameterizations using novel conservative and volatile tracers. Global Biogeochem. Cy. 14 (1), 373–387. https://doi.org/10.1029/1999gb900091.

Park, K.-T., Lee, K., Kim, T.-W., Yoon, Y.J., Jang, E.-H., Jang, S., Lee, B.-Y., Hermansen, O., 2018. Atmospheric DMS in the Arctic Ocean and Its Relation to Phytoplankton Biomass. Global Biogeochem. Cy. 32 (3), 351–359. https://doi.org/10.1002/2017GB005805.

Park, K.-T., Lee, K., Yoon, Y.-J., Lee, H.-W., Kim, H.-C., Lee, B.-Y., Hermansen, O., Kim, T.-W., Holmén, K., 2013. Linking atmospheric dimethyl sulfide and the Arctic Ocean spring bloom. Geophys. Res. Lett. 40 (1), 155–160. https://doi.org/10.1029/2012GL054560.

Preunkert, S., Jourdain, B., Legrand, M., Udisti, R., Becagli, S., Cerri, O., 2008. Seasonality of sulfur species (dimethyl sulfide, sulfate, and methanesulfonate) in Antarctica: Inland versus coastal regions. J. Geophys. Res. 113 (D15), D15302. https://doi.org/10.1029/2008JD009937.

Preunkert, S., Legrand, M., Jourdain, B., Moulin, C., Belviso, S., Kasamatsu, N., Fukuchi, M., Hirawake, T., 2007. Interannual variability of dimethylsulfide in air and seawater and its atmospheric oxidation by-products (methanesulfonate and sulfate) at Dumont d'Urville, coastal Antarctica (1999–2003). J. Geophys. Res. 112 (D6), D06306. https://doi.org/10.1029/2006JD007585.

Quinn, P., Bates, T., 2011. The case against climate regulation via oceanic phytoplankton sulphur emissions. Nature 480 (7375), 51–56. https://doi.org/10.1038/nature10580.

Quinn, P.K., Coffman, D.J., Johnson, J.E., Upchurch, L.M., Bates, T.S., 2017. Small fraction of marine cloud condensation nuclei made up of sea spray aerosol. Nat. Geosci. 10, 674–679. https://doi.org/10.1038/ngeo3003.

Read, K., Lewis, A., Bauguitte, S., Rankin, A.M., Salmon, R., Wolff, E.W., Saiz-Lopez, A., Bloss, W., Heard, D., Lee, J., 2008. DMS and MSA measurements in the Antarctic Boundary Layer: impact of BrO on MSA production. Atmos. Chem. Phys. 8 (11), 2985–2997. https://doi.org/10.5194/acp-8-2985-2008.

Saltzman, E.S., King, D.B., Holmen, K., Leck, C., 1993. Experimental Determination of the Diffusion Coefficient of Dimethylsulfide in Water. J. Geophys. Res. 98 (C9), 16481–16486. https://doi.org/10.1029/93JC01858.

Saltzman, E., De Bruyn, W., Lawler, M., Marandino, C., McCormick, C., 2009. A chemical ionization mass spectrometer for continuous underway shipboard analysis of dimethylsulfide in near-surface seawater. Ocean Sci. 5, 537–546. https://doi.org/10.5194/os-5-537-2009.

Simo, R., Dachs, J., 2002. Global ocean emission of dimethylsulfide predicted from biogeophysical data. Global Biogeochem. Cy. 16 (4). https://doi.org/10.1029/2001GB001829. 26.21-26.10.

Spreen, G., Kaleschke, L., Heygster, G., 2008. Sea ice remote sensing using AMSR-E 89-GHz channels. J. Geophys. Res.-Oceans 1978–2012https://doi.org/10.1029/2005JC003384. 113(C2).

Staubes, R., Georgii, H.W., 1993. Biogenic sulfur compounds in seawater and the atmosphere of the Antarctic region. Tellus B 45 (2), 127–137. https://doi.org/10.1034/j.1600-0889.1993.t01-1-00005.x.

Stefels, J., Steinke, M., Turner, S., Malin, G., Belviso, S., 2007. Environmental constraints on the production and removal of the climatically active gas dimethylsulfide (DMS) and implications for ecosystem modelling. Biogeochemistry 83 (1), 245–275. https://doi.org/10.1007/978-1-4020-6214-8_18.

Tortell, P., Gueguen, C., Long, M., Payne, C., Lee, P., DiTullio, G., 2011. Spatial variability and temporal dynamics of surface water pCO_2, Δ_O2/Ar and dimethylsulfide in the Ross Sea Antarctica. Deep Sea Res. Pt I: Oceanogr. Res. Pap. 58, 241–259. https://doi.org/10.1016/j.dsr.2010.12.006.

Tortell, P.D., Long, M.C., 2009. Spatial and temporal variability of biogenic gases during

the Southern Ocean spring bloom. Geophys. Res. Lett. 36 (1), L01603. https://doi.org/10.1029/2008GL035819.

Tortell, P.D., Long, M.C., Payne, C.D., Alderkamp, A.C., Dutrieux, P., Arrigo, K.R., 2012. Spatial distribution of pCO_2, ΔO_2/Ar and dimethylsulfide (DMS) in polynya waters and the sea ice zone of the Amundsen Sea, Antarctica, Deep Sea Res Pt II: Top. Stud. Oceanogr 71–76, 77–93. https://doi.org/10.1016/j.dsr2.2012.03. 010.

Trevena, A., Jones, G., 2012. DMS flux over the Antarctic Sea Ice Zone. Mar. Chem. 134–135, 47–58. https://doi.org/10.1016/j.marchem.2012.03.001.

Vallina, S.M., Simó, R., Gassó, S., 2006. What controls CCN seasonality in the Southern Ocean? A statistical analysis based on satellite-derived chlorophyll and CCN and model-estimated OH radical and rainfall. Global Biogeochem. Cy 20 (1), GB1014. https://doi.org/10.1029/2005GB002597.

Vogt, M., Liss, P., 2009. Dimethylsulfide and climate. Geophys. Monogr. Ser. 187, 197–232. https://doi.org/10.1029/2008GM000790.

Yang, G.-P., Zhuang, G.-C., Zhang, H.-H., Dong, Y., Yang, J., 2012. Distribution of dimethylsulfide and dimethylsulfoniopropionate in the Yellow Sea and the East China Sea during spring: Spatio-temporal variability and controlling factors. Mar. Chem. 138, 21–31. https://doi.org/10.1016/j.marchem.2012.05.003.

Yokouchi, Y., Li, H.J., Machida, T., Aoki, S., Akimoto, H., 1999. Isoprene in the marine boundary layer (southeast Asian Sea, eastern Indian Ocean, and Southern Ocean): Comparison with dimethyl sulfide and bromoform. J. Geophys. Res.-Atmospheres 104 (D7), 8067–8076. https://doi.org/10.1029/1998jd100013.

Zhang, M., Marandino, C.A., Chen, L., Sun, H., Gao, Z., Park, K., Kim, I., Yang, B., Zhu, T., Yan, J., Wang, J., 2017. Characteristics of the surface water DMS and pCO2 distributions and their relationships in the Southern Ocean, southeast Indian Ocean, and northwest Pacific Ocean. Global Biogeochem. Cy 31 (8), 1318–1331. https://doi.org/10.1002/2017gb005637.

Zhang, M., Gao, W., Yan, J., Wu, Y., Marandino, C.A., Park, K., Chen, L., Lin, Q., Tan, G., Pang, M., 2019. An integrated sampler for shipboard underway measurement of dimethyl sulfide in surface seawater and air. Atmos. Environ. 209, 86–91. https://doi.org/10.1016/j.atmosenv.2019.04.022.